THE JOURNAL OF PHYSICAL CHEMISTRY B

Article

pubs.acs.org/JPCB

Kinetic Studies of Amino Acid-Based Surfactant Binding to DNA

Deenan Santhiya,[†,#] Rita S. Dias,*[,‡] Sounak Dutta,[§] Prasanta Kumar Das,*[,§] Maria G. Miguel,[‡] Björn Lindman,[‡,∥] and Souvik Maiti*[,†,⊥]

[†]Institute of Genomics and Integrative Biology, CSIR, Mall Road, Delhi 110007, India

[‡]Department of Chemistry, University of Coimbra, Rua Larga, 3004-535 Coimbra, Portugal

[§]Department of Biological Chemistry, Indian Association for the Cultivation of Science, Jadavpur, Kolkata 700032, India

[∥]Physical Chemistry, Department of Chemistry, Lund University, P.O. Box 124, S-22100 Lund, Sweden

[⊥]National Chemical Laboratory, CSIR, Dr. Homi Bhabha Road, Pune 411008, India

ABSTRACT: In this work, the binding kinetics of amino acid-based surfactants, presenting different linkers and head groups, with calf thymus (CT)-DNA was studied using stopped-flow fluorescence spectroscopy. The kinetic studies were carried out as a function of Na^+ concentration and surfactant-to-DNA charge ratio. The surfactant binding on DNA took place in two consecutive steps, for which the corresponding first and second relative rate constants (k_1 and k_2) were determined. The fast step was attributed to the surfactant binding to DNA and micelle formation in its vicinity, the slower step to DNA condensation and possible rearrangement of the surfactant aggregates. In general, both relative rate constants increase with surfactant concentration and decrease with the ionic strength of the medium. The architecture of the surfactant was found to have a significant impact on the kinetics of the DNA−surfactant complexation. Surfactants with amide linkers showed larger relative rate constants than those with ester linkers. The variation of the relative rate constants with the head groups of the surfactants, alanine and proline, was found to be less obvious, being partially dependent on the surfactant concentration.

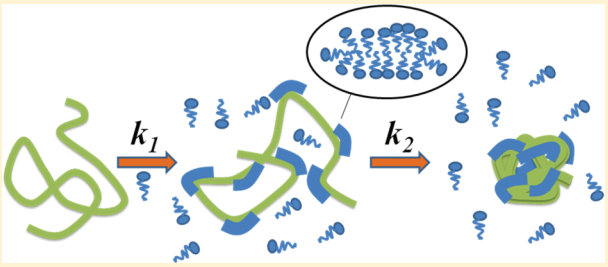

INTRODUCTION

Numerous researchers claim that nonviral vectors (e.g., cationic surfactants, lipids, polymers, dendrimers, and peptides) present more advantages than viral vectors for the delivery of nucleic acid (DNA, RNA) into specific cells (gene delivery).[1−7] Gene delivery is a potential therapeutic method for treating a wide variety of diseases, including inherited disorders such as cystic fibrosis, Parkinson, cardiovascular diseases, and many others.[4,7] It is also an alternative method to traditional chemotherapy used in treating cancer.[8]

The first step in the preparation of gene vehicles involves the condensation of the nucleic acid. This can be achieved resorting to multivalent agents, such as polycations, cationic lipids, and surfactants.[4] Another crucial step in gene delivery is the dissociation of such nucleic acid-based cationic complexes in the cytoplasm of the target cell. The lack of dissociation of the vehicle results in a deficient transfection efficiency,[9] while the prematurely released nucleic acids is known to be rapidly degraded by serum nuclease in the blood. Hence it is important that the interactions between the nucleic acid and the cationic vector be well balanced. In addition to this, facile cellular uptake of a nucleic acid via plasma membrane permeation depends on its size and charge.[4,7] The size and charge of the complex can be controlled by using vectors with specific architectures, which implies that the prediction of in vitro and in vivo gene transfection efficiency can, in principle, be based solely on the physicochemical characteristics of these nanocomplexes.[4,7] The interaction between cationic vectors and nucleic acids has thus been extensively studied using a range of experimental and simulation techniques.[4,10]

Recent investigations of amino acid-based copolymers as gene delivery agents show that their composition have an impact on the protection of nucleic acids against degradation by nuclease, as well as on cytotoxicity and transfection efficiency.[11,12] Additionally, surfactant architecture, via its influence on surfactant self-assembly, is well-known to affect the nucleic acid compaction and decompaction process.[4] These facts have motivated us to study the interactions between DNA and amino acid-based surfactant molecules of varied architecture (head, linker, and tail groups) through biophysical studies such as gel electrophoresis, ethidium bromide (EB) exclusion assays, circular dichroism, and UV melting temperature determination.[13−15] For example, interaction studies were carried out between plasmid DNA and amino acid-based surfactants with headgroups presenting different hydrophobicities (alanine, proline, and phenylalanine). Interestingly, the surfactants with more complex/bulkier hydrophobic headgroups (phenylalanine) interacted more strongly with DNA and also presented lower cytotoxicity even at relatively high surfactant concentrations.[13] The effect of tail length on the

Received: February 2, 2012
Revised: April 30, 2012
Published: May 3, 2012

   dx.doi.org/10.1021/jp301069t | J. Phys. Chem. B 2012, 116, 5831−5837

condensation of 14-mer double-stranded DNA was monitored, revealing that, as with longer DNA chains,[16] a smaller amount of the longer chain length surfactant was required to achieve DNA-induced self-assembly.[14] A recent investigation on the interaction between DNA and amino acid-based surfactants with different linker groups showed a strong interaction of the amide linker with DNA when compared to ester linker.[15] These findings suggest that the degree of control achieved with surfactants of different architectures makes them a promising precompacting agent of DNA for gene delivery applications. Furthermore, we are interested in extending our studies by investigating kinetic parameters that characterize the formation of DNA−surfactant complexes, and how such parameters vary with the architecture of the surfactants.

Kinetic studies of similar systems have been performed using ion-selective electrodes,[17] potentiometry,[18] stopped-flow fluorescence,[19−22] and circular dichroism.[20] In this work, we used stopped-flow fluorescence to follow the kinetics of the interaction of four amino acid-based surfactants, carrying two different linkers and headgroups, with calf thymus (CT)-DNA. Besides the effect of surfactant architecture, we have looked into the surfactant-to-DNA charge ratio and ionic strength.

MATERIALS AND METHODS

Materials. Highly polymerized, fibrously prepared sodium salt form of CT-DNA (CAS 73049-39-5), from Sigma, was used as received. Stock CT-DNA solutions were prepared as follows: the required amount of DNA fibers was dissolved in 10 mL of 10 mM sodium phosphate buffer solution (pH = 7.0) in a 50 mL vial and kept in an orbital shaker (Thermo scientific) at 180−220 rpm overnight at 37 °C. The concentration (in phosphate groups) of the DNA stock solutions was measured spectrophotometrically considering the molar extinction coefficient of the DNA base pairs to be equal to 6600 M^{-1} cm^{-1}.[23] The ratio of the absorbance at 260 and 280 nm was found to be 1.8. Further, a negligible absorbance was observed at 320 nm, indicating the absence of protein contamination. The transition temperature (T_m) of CT-DNA was found to be 85 °C using Cary 100 concentration UV−visible spectrophotometer with temperature controller, in good agreement with the information provided by Sigma. The B-form of DNA in solution was confirmed by the appearance of a positive peak at 273 nm and a negative peak at 245 nm using circular dichroism (Jasco spectropolarimeter model 715). The spectrum was recorded between 220 and 325 nm.

EB was purchased from Sigma, and its stock solution was prepared by dissolving 1.97 mg in 1000 μL of buffer. The concentration was determined using a UV−visible spectrophotometer assuming a molar extinction coefficient of 5600 L mol^{-1} cm^{-1} at 480 nm[24] and stored in the dark at 4 °C.

The following four different surfactants were used to study the kinetics of the interactions between CT-DNA and surfactant:

(i) *2-Hexadecylcarbamoyl-1,1-dimethyl-pyrrolidinium chloride (amide-pro).* δ = 0.86 (t,3H), 1.16−1.30 (br, 28H), 1.561−1.61(br, 4H), 3.21−3.26 (m, 2H), 3.28(s, 3H), 3.39(s, 3H) 3.49−3.55 (m, 2H), 5.60 (t, 1H). Elemental analysis: Calculated for $C_{23}H_{47}N_2OCl$: C, 68.53: H, 11.75; N, 6.95. Found: C, 68.23; H, 11.61; N, 6.65. MS (ESI) caled.m/z = 367.3688; found 367.4124 (M^+).

(ii) *2-Hexadecyloxycarbamoyl-1,1-dimethyl-pyrrolidinium chloride (ester-pro).* δ = 0.88 (t, 3H), 1.33−1.18 (m, 28H), 1.70−1.63(br, 4H), 3.19 (s, 3H), 3.74 (s, 3H), 3.88 (m, 2H), 4.27−4.17 (m, 2H), 5.44 (t, 1H). Elemental analysis: Calculated for $C_{23}H_{46}ClNO_2$: C, 68.37; H, 11.47; N, 3.47. Found: C, 68.71; H, 11.35; N, 3.61. MS (ESI) caled.m/z = 368.3529; found 368.3229 (M^+).

(iii) *(1-Hexadecylcarbamoyl-ethyl)-trimethyl-ammonium chloride (amide-ala).* δ = 0.87 (t, 3H), 1.24−1.16 (br, 26H), 1.61−1.56 (d, 3H), 1.74 (br, 2H), 3.28−3.21(m, 2H), 3.33 (s, 9H), 5.69−5.65 (t, 1H). Elemental analysis: Calculated for $C_{22}H_{47}N_2OCl$: C, 67.57; H, 12.11; N, 7.16. Found: C, 67.41; H, 11.79; N, 6.91. MS (ESI) caled.m/z = 355.3688; found 355.1259 (M^+).

(iv) *(1-Hexadecyloxycarbonyl-ethyl)-trimethyl-ammonium chloride (ester-ala).* δ = 0.88 (t, J = 5.58, 3H), 1.33−1.18 (m, 28H), 1.75 (m, 3H), 3.59 (s, 9H), 4.27−4.19 (br, 2H), 4.87 (q, J = 7.17 Hz, 1H). Elemental analysis: Calculated for $C_{22}H_{46}ClNO_2$: C, 67.40; H, 11.83; N, 3.57. Found: C, 67.31; H, 11.65; N, 3.45. MS (ESI) caled.m/z = 356.3529; found 356.3622 (M^+).

The syntheses, as well as the determination of cmc values of these surfactants, are described elsewhere.[15] The surfactant stock solutions were prepared by dissolving a known amount of surfactant in a required volume of warm sodium phosphate buffer solution. The corresponding concentrations were determined gravimetrically. Structures and cmc values of the surfactants under study are shown in Figure 1.

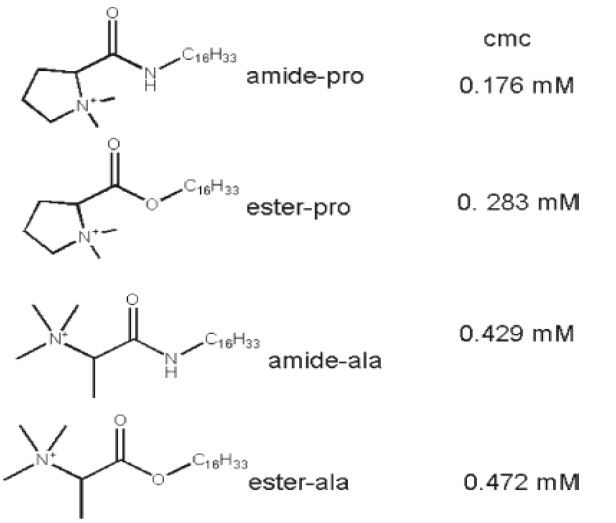

Figure 1. Structures and cmc values (determined in water) of the surfactants under study: (a) amide-pro, (b) ester-pro, (c) amide-ala, and (d) ester-ala.

All the experiments were carried out using 10 mM sodium phosphate buffer at pH 7.0, prepared from Milli-Q water. The other reagents used in this study were of AR-grade purity.

Steady-State Fluorescence Spectroscopic Studies. Fluorescence spectra of the CT-DNA−EB complex were recorded in the absence and presence of various amino acid-based surfactants (amide-pro, amide-ala, ester-pro and ester-ala) from 500 to 700 nm, at an excitation wavelength (λ_{ex}) of 480 nm. The required amount of EB was mixed with 25 μM DNA solutions (1EB:1bp) in the sodium phosphate buffer and equilibrated for 10 min at 25 °C. The CT-DNA−EB mixture (600 μL) was placed in a cuvette, and aliquots of the desired surfactant solution were added to the mixture. After each addition of surfactant, the mixture was incubated for 10 min

dx.doi.org/10.1021/jp301069t | J. Phys. Chem. B 2012, 116, 5831−5837

before recording the spectrum. The dilution of DNA was kept below 10%, and the surfactant-to-DNA charge ratio, $Z_{\pm}$, was calculated taking into account the dilution factor.

Stopped-Flow Fluorescence Spectroscopic Studies. Stopped-flow fluorescence spectroscopic experiments were performed using a SFA-20 rapid kinetics accessory (HI-Tech Scientific) in a spectrofluorometer (JobinYvonFluoroMax 3) with a Peltier thermostat. Solutions with 25 μM CT-DNA and the various surfactants at three different concentrations (25, 75, and 225 μM) were prepared. The charge ratio of such solutions was $Z_{\pm}$ = 1, 3, and 9, respectively. Since EB was the fluorescent probe, the excitation and emission monochromators were set to 480 and 590 nm, respectively. The temperature was maintained at 25 °C. During the procedure, the CT-DNA–EB mixture and the surfactant solution with the desired concentrations were taken in two separate syringes of the stopped-flow setup and injected at once into the sample holder. The EB emission was monitored continuously both before (t = 0 s) and after the injection. Additionally, experiments were carried out with increasing concentrations of sodium ions (16 (sodium phosphate buffer only), 41, 66, 116, and 166 mM). The dead time of the instrument was determined from the test reaction described elsewhere,[25] and estimated to 5 ms for a 1:1 mixing. Suitable control experiments were carried out by mixing a CT-DNA–EB solution and buffer solutions (with and without extra Na^+); the EB signal was found to be unchanged within the time of the measurement.

RESULTS AND DISCUSSION

To investigate surfactant binding to DNA, we started by performing steady-state fluorescence studies using EB and, afterward, looked into the kinetics of CT-DNA–surfactant complexation as a function of $Z_{\pm}$, salt concentration, and surfactant architecture.

DNA–Surfactant Complexation. Steady-state fluorescence spectroscopic studies were performed to monitor the DNA–surfactant complexation. Figure 2a–d portrays fluorescence emission spectra of free EB, the CT-DNA–EB complex, and the CT-DNA–surfactant complex for the different surfactants (amide pro, amide ala, ester pro, and ester ala, respectively) at various $Z_{\pm}$ and at 16 mM Na^+ (sodium phosphate buffer contribution only). Traces 1 and 2 in Figure 2 show the spectra of free EB and EB bound to CT-DNA, respectively. It is clearly seen that the association of EB with CT-DNA leads to a significant increase in fluorescence emission of ethidium ions at 590 nm, upon excitation at 480 nm.[26] Cationic ligands are known to displace the EB molecules that are intercalated between the DNA base pairs, inducing a decrease in the fluorescence of EB. The EB exclusion method is, thus, a commonly used tool for probing native DNA molecules as well as the degree of interaction between those and cationic vectors.[13−15,27] The extent of EB displacement depends both on the characteristics of the cationic ligands and the strength of their interaction with DNA. The arrows in Figure 2 show the decrease of fluorescence intensity upon increase of the surfactant concentration. All surfactants under study induce some release of EB. For the amide-ala surfactant, a striking initial decrease in the fluorescence was observed at a surfactant-to-DNA charge ratio $Z_{\pm}$ = 1, followed by a very small or negligible fluorescence decrease at higher charge ratios ($Z_{\pm}$ = 3, 9, and 12). The same behavior was found for ester-ala, but the initial fluorescence decrease was more moderate. Regarding the pro surfactants, the intensity decrease was more gradual, and the saturation was achieved at higher charge ratios ($Z_{\pm}$ > 3). This is in good agreement with previous observations.[15]

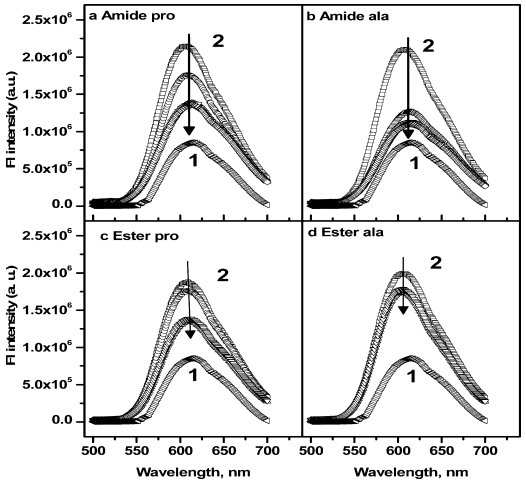

Figure 2. EB fluorescence spectra for (a) amide-pro, (b) amide-ala, (c) ester-pro ,and (d) ester-ala. Traces 1 and 2 in each plot are fluorescence emission spectra of free EB and EB bound to CT-DNA. The down arrows indicate the increase of $Z_{\pm}$. The CT-DNA concentration was 25 μM in 10 mM sodium phosphate buffer (16 mM Na^+, pH 7.0).

The binding kinetics of the amino acid-based cationic surfactant–DNA complexation was studied by following the EB exclusion with time. This methodology has been successfully used by Barreleiro et al. to study DNA–cationic vesicle complexation, in the development of nonviral gene delivery systems.[19]

Figure 3a shows a typical fluorescence intensity decay of EB observed upon amide-pro surfactant binding to CT-DNA at $Z_{\pm}$ = 1, in the presence of 66 mM Na^+ ions. The kinetic curve was analyzed assuming that the fluorescence curve is a superposition of exponentials terms, according to

$$I(t) = \sum_{i=1}^{i} A_i \exp(-k_i t) \quad (1)$$

where I is the fluorescence at time t, A_i is the prefactors, and k_i is the relative rate constants. The Nelder–Mead simplex method for minimizing eq 1 was applied. The quality of the fit was assessed from the χ^2 value. The number of exponentials was increased until no systematic deviation of the residual was found (Figure 3b). It was found that two exponential functions (i = 2) were sufficient to describe the fluorescence decay kinetics of EB upon amide-pro surfactant binding to CT-DNA.

These observations are in good agreement with earlier reports showing a two-step mechanism for the binding kinetics of cetyltrimethylammonium bromide (CTAB),[18] lipids,[20] and dendrimers[20] to DNA. It is generally accepted in the literature that the two steps are assigned to (i) the binding of the condensing agent and potential dehydration of the phosphate groups of DNA and/or the positively charged groups of the condensing agents, followed by (ii) the condensation of the DNA. DNA condensation in the presence of oppositely charged surfactants occurs as a result of the formation of surfactant aggregates in the vicinity of the macromolecule, as demonstrated by the sigmoidal shape (cooperative binding) of the binding isotherms[28,29] and the presence of liquid crystalline

dx.doi.org/10.1021/jp301069t | J. Phys. Chem. B 2012, 116, 5831−5837

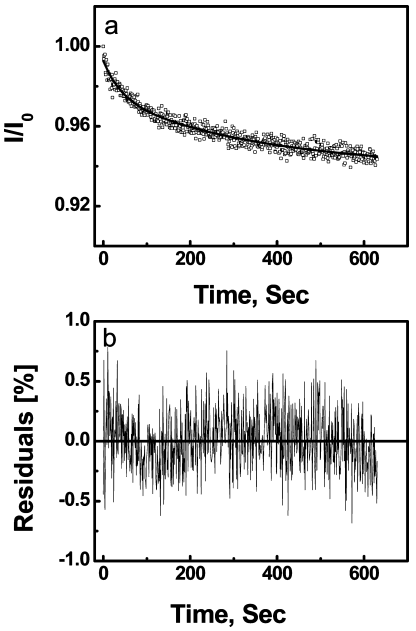

Figure 3. (a) Stopped-flow data corresponding to the fluorescence intensity decay of EB observed upon amide-pro binding to CT-DNA at $Z_{\pm} = 1$, in the presence of 66 mM Na^+, as a function of time. The CT-DNA concentration was 25 μM in 10 mM sodium phosphate buffer (pH 7.0). The smooth line in panel a shows the fitting obtained with eq 1 and panel b shows the residuals of the fit.

phases[4] in these systems. The surfactant concentration at which the aggregates are formed, the so-called critical association constant (cac), is well below the surfactant critical micellar concentration (cmc), due to the presence of the highly charged polyelectrolyte. This is a very common phenomenon in polyelectrolyte−oppositely charged surfactant systems.[30] The surfactant aggregates act as multivalent species that induce attractive interactions between and within the DNA chains, due to ion correlation effects.[31] It was, however, not clear from the literature which of the steps corresponds to aggregate (e.g., micelle) formation in the vicinity of the DNA.[18] With vicinity we imply that, although the surfactant micelles are adsorbed onto the DNA chain, both DNA and surfactants retain some hydration. We believe that step I in the DNA−surfactant interaction is due to the binding of surfactant and formation of surfactant micelles (see below), whereas step II is due to the condensation of the DNA, induced by the presence of the surfactant aggregates (Figure 4). During the latter process, it is also possible that some rearrangement, in terms of size and shape, occurs in the surfactant micelles. Additionally, in the present case, one should also consider the EB displacement from the DNA molecules. The reaction scheme is as follows:

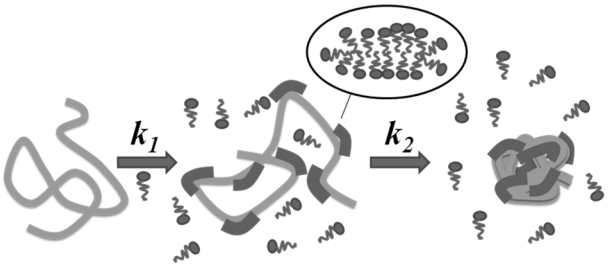

Figure 4. Schematic representation of the proposed surfactant binding mechanism and DNA compaction. The different components are not at scale.

$$S^+ + DNA{-}EB \leftrightarrow DNA{-}S + EB$$

which can be divided in three reactions:

$$DNA{-}EB \leftrightarrow DNA + EB$$

$$DNA + S^+ \underset{k_1}{\leftrightarrow} DNA{-}S(rc)$$

$$DNA{-}S(rc) \underset{k_2}{\leftrightarrow} DNA{-}S(cs)$$

where 'rc' stands for random coil and 'cs' is for compacted state.

Previous kinetic studies on the interactions of DNA with cationic surfactants performed in the absence of a fluorescence dye strongly suggest that the two rate constants found in this work correspond to the binding process of the surfactants to DNA. It is likely that the EB displacement of the DNA molecules affects the rate constants; however, it is difficult to separate the contributions since the surfactants bind to DNA as micelles and EB binds to it individually. In fact, it has been shown that different fluorescence probes give rise to differences in both constant rates that describe the binding of cationic dendrimers and lipids to DNA.[20] Nevertheless, the EB displacement mechanism from DNA is not expected to vary with the different surfactants and, thus, the differences in the rate constants arise due to the variations in surfactant structure. It should be noted, thus, that this methodology provides relative rate constants.

Considering this mechanism it is likely that the relative rate constants vary with the ionic strength of the medium, surfactant concentrations, as well as the architecture of the surfactants. The latter, having an impact on the shape and size of the micelles, can affect DNA compaction and accessability.[4,32]

Effect of Charge Ratio on the Binding Kinetics. Figure 5 shows plots of the fluorescence intensity versus time for each of the three surfactant-to-DNA charge ratios and for the different surfactants. The rate of binding is found to be fast initially and, the higher the charge ratio, the higher was the initial rate. As in the example shown above, the fluorescence emission fits into a biexponential function, indicating a two-step process. The fluorescence decay is larger for lower charge ratios for all surfactants under study. The observed relative rate constants, k_1 and k_2, as a function of the charge ratio, for the four surfactants under study are shown in Table 1. Each rate constant is an average of three independent kinetic experiments.

It can be seen that, for all surfactants under study, the relative rate constants are well separated, by at least an order of magnitude, and, in general, increase with increasing charge ratio.

As discussed above, the first step is due to the electrostatic binding of the surfactant cations to the DNA, which is a diffusion-driven process. As such, the larger the amount of added surfactant, the faster the reaction will progress. The fact that k_1 is different for all surfactants shows that micelle formation occurs at this step, since the diffusion (and binding) of individual surfactants would not lead to such large differences in the relative rate constant of the different surfactants. The second relative rate constant also varies with the concentration of surfactant for most of the studied systems, although the variations are smaller than for k_1. The condensation of DNA occurs upon the formation of surfactant

dx.doi.org/10.1021/jp301069t | J. Phys. Chem. B 2012, 116, 5831−5837

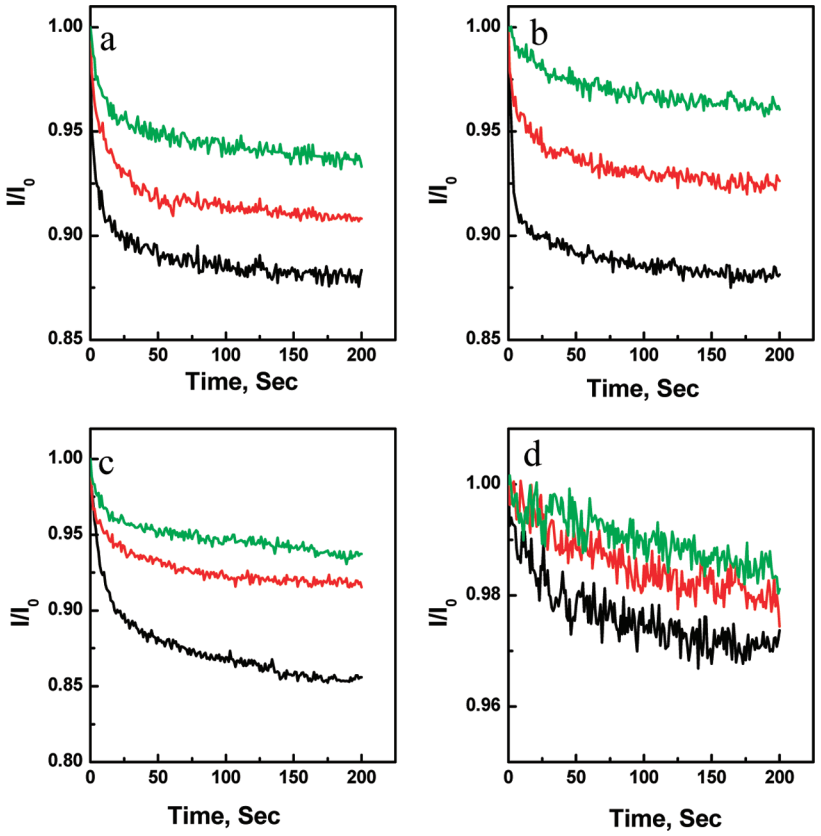

Figure 5. Fluorescence intensity as a function of time for (a) amide-pro, (b) amide-ala, (c) ester-pro, and (d) ester-ala binding to CT-DNA at $Z_{\pm} = 1$ (black), 3 (red) and 9 (green) and at 166 mM Na^+ concentration. The CT-DNA concentration was 25 μM in 10 mM sodium phosphate buffer (pH 7.0).

Table 1. Relative Rate Constants for the Different Cationic Surfactants Binding to CT-DNA as a Function of the Charge Ratio, $Z_{\pm}$, for Two Different Na^+ Concentrations

		16 mM Na^+		166 mM Na^+	
surfactant	$Z_{\pm}$	k_1 (s^{-1})	k_2 (s^{-1})	k_1 (s^{-1})	k_2 (s^{-1})
Amide-pro	1.0	$0.303 \pm 1 \times 10^{-3}$	$0.021 \pm 1 \times 10^{-4}$	$0.118 \pm 2 \times 10^{-3}$	$0.003 \pm 2 \times 10^{-4}$
	3.0	$0.431 \pm 5 \times 10^{-3}$	$0.025 \pm 2 \times 10^{-4}$	$0.135 \pm 0.4 \times 10^{-3}$	$0.008 \pm 3 \times 10^{-4}$
	9.0	$0.580 \pm 0.2 \times 10^{-3}$	$0.033 \pm 1 \times 10^{-4}$	$0.183 \pm 1 \times 10^{-3}$	$0.009 \pm 2 \times 10^{-4}$
Amide-ala	1.0	$0.099 \pm 4 \times 10^{-3}$	$0.005 \pm 2 \times 10^{-4}$	$0.036 \pm 2 \times 10^{-3}$	$0.001 \pm 0.4 \times 10^{-4}$
	3.0	$0.130 \pm 3 \times 10^{-3}$	$0.005 \pm 5 \times 10^{-4}$	$0.048 \pm 2 \times 10^{-3}$	$0.002 \pm 0.9 \times 10^{-4}$
	9.0	$0.174 \pm 9 \times 10^{-3}$	$0.009 \pm 1 \times 10^{-4}$	$0.059 \pm 0.8 \times 10^{-3}$	$0.003 \pm 0.4 \times 10^{-4}$
Ester-pro	1.0	$0.037 \pm 6 \times 10^{-3}$	$0.003 \pm 0.2 \times 10^{-4}$	$0.035 \pm 0.5 \times 10^{-3}$	$0.003 \pm 1 \times 10^{-4}$
	3.0	$0.057 \pm 0.4 \times 10^{-3}$	$0.004 \pm 1 \times 10^{-4}$	$0.060 \pm 0.3 \times 10^{-3}$	$0.003 \pm 1 \times 10^{-4}$
	9.0	$0.069 \pm 0.2 \times 10^{-3}$	$0.005 \pm 1 \times 10^{-4}$	$0.076 \pm 0.5 \times 10^{-3}$	$0.004 \pm 1 \times 10^{-4}$
Ester-ala	1.0	$0.042 \pm 0.9 \times 10^{-3}$	$0.0046 \pm 0.3 \times 10^{-4}$	$0.042 \pm 0.3 \times 10^{-3}$	$0.0044 \pm 4 \times 10^{-4}$
	3.0	$0.052 \pm 0.1 \times 10^{-3}$	$0.0044 \pm 0.9 \times 10^{-4}$	$0.049 \pm 0.7 \times 10^{-3}$	$0.0044 \pm 7 \times 10^{-4}$
	9.0	$0.049 \pm 0.5 \times 10^{-3}$	$0.0044 \pm 0.7 \times 10^{-4}$	$0.050 \pm 0.7 \times 10^{-3}$	$0.0045 \pm 3 \times 10^{-4}$

micelles in its vicinity and is, therefore, expected to follow the same trend.

We can also see from Table 1 that the amide-pro surfactant shows the largest variations of k_1 and k_2 with surfactant concentration, as opposed to the ester-ala surfactant that shows only a small increase in k_1 when the mixing ratio is increased from $Z_{\pm} = 1-3$, and no significant variation of k_2 for all studied $Z_{\pm}$. This particular surfactant showed, indeed, a much smaller release of EB in the steady-state fluorescence studies, which indicates that its binding to DNA is weaker than the other surfactants considered. Further considerations on the surfactant architecture and its influence on DNA condensation are presented below. In Table 1 are also compiled the relative rate constants as a function of $Z_{\pm}$ for larger concentrations of salt, $[Na^+] = 166$ mM. Again, two separate rate constants are found for each system the values of which increase with the concentration of surfactant. This increase is, however, much less pronounced and, again, ester-ala shows the least variation. It can also be seen that the relative rate constants have a smaller magnitude when the salt concentration is increased.

Effect of Salt Concentration on Kinetics. We have looked more carefully at the effect of the salt concentration on the kinetics of CT-DNA–cationic surfactant complexation. The results are compiled in Figures 6 and 7. For the surfactants with

dx.doi.org/10.1021/jp301069t | J. Phys. Chem. B 2012, 116, 5831–5837

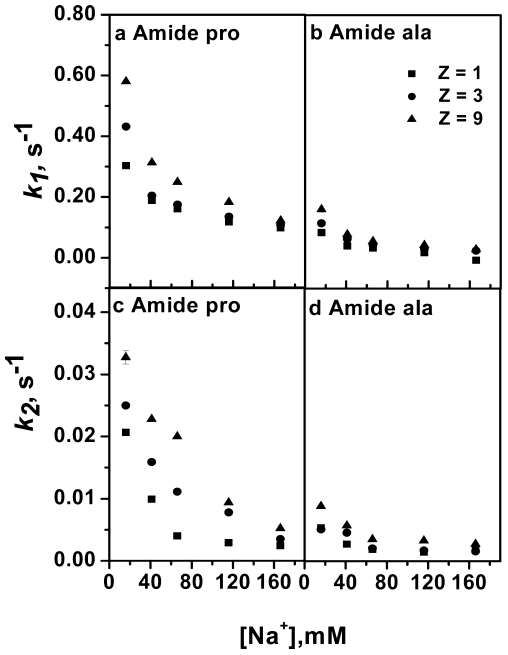

Figure 6. First and second relative rate constants (k_1 and k_2) for (a,c) amide-pro and (b,d) amide-ala binding to CT-DNA, respectively, as a function of Na^+ concentration at various charge ratios. The CT-DNA concentration was 25 μM in 10 mM sodium phosphate buffer (pH 7.0).

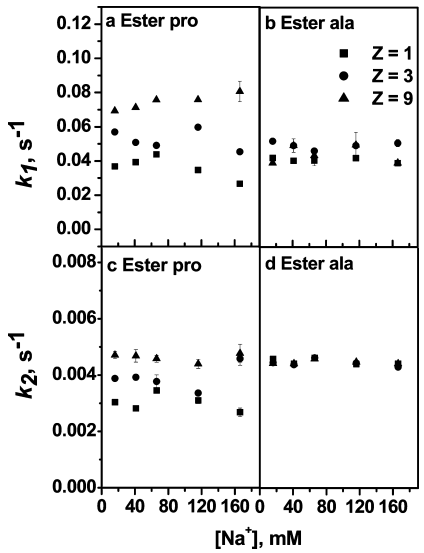

Figure 7. First and second relative rate constants (k_1 and k_2) for (a,c) ester-pro and (b,d) ester-ala binding on CT-DNA, respectively, as a function of Na^+ concentration at various charge ratios. The CT-DNA concentration was 25 μM in 10 mM sodium phosphate buffer (pH 7.0).

the amide linker (Figure 7), there is a decrease in both relative rate constants with increasing the concentration of salt, for all considered $Z_{\pm}$ values, even though the decrease is more moderate for $Z_{\pm}$ = 1.0. As a result, the relative rate constants for the different charge ratios for large concentrations of salt are very similar. The decrease in the rate constants with increasing ionic strength is expected since the interactions between DNA and the cationic surfactants, that are primarily electrostatic in nature, will be screened. The same has been observed for DNA–CTAB systems.[18] The ester-linker surfactants, on the other hand, show a different behavior upon variations of the salt concentration (Figure 7). For the DNA–ester-pro systems, and all studied charge ratios, the obtained relative rate constants present some fluctuations with the concentration of salt; however, the general behavior shows no significant variations of k_1 and k_2 with salt concentration. For the ester-ala surfactant, and as observed for variations in the charge ratio (also depicted in Figure 7), there is no dependence of the relative rate constants on the salt concentration. This is, again, indicative of the weaker interaction of this surfactant with DNA.

Effect of Surfactant Architecture on Kinetics. It is clear from the results shown here that there is a significant difference in the binding of the cationic surfactants to DNA when amide or ester linkers are used. Surfactants with amide linkers (amide-pro and amide-ala) show larger relative rate constants, as well as larger variations of the relative rate constants with surfactant-to-DNA charge ratio, $Z_{\pm}$, and salt concentration. All of this indicates a stronger binding of the surfactants to DNA, as previously observed.[15] This is probably related to the possibility of amide linkers to form hydrogen bonds between the different surfactant molecules.[32] Hydrogen-bonding is facilitated in a nonpolar environment and will act to favor the aggregation of surfactants and stabilization of the micelles. Note that the cmc of the amide-linker surfactants is lower than that of the corresponding surfactants with the ester linker (Figure 1). The amide surfactants can also potentially form hydrogen bonds with the bases of DNA; however, there is no evidence of a decrease in the cooperativity of the binding of surfactant, which would be expected if the binding of individual surfactant molecules to DNA was significant. Surfactants with ester groups in the linker have, on the other hand, lower relative rate constants, smaller variations of the relative rate constants, and nearly no variations with the salt concentration, which indicates a weaker interaction between those surfactants and DNA. The ester group has been reported to be more flexible than the amide group,[32] which may decrease the interactions of the surfactant molecules to the DNA, since their association restricts the conformation of the surfactant, leading to a loss in entropy.

Regarding the headgroups of the surfactants, we have considered two different types of headgroups, the proline (pro) and the alanine (ala) groups. When surfactants with the amide linker are considered, it is observed that both relative rate constants are larger for the proline headgroup, for all considered charge ratios and salt concentrations, an indication that the proline groups interact more strongly with the DNA. This is in good agreement with our previous results[13] in which isothermal titration calorimetry (ITC) experiments showed, upon the interaction with plasmid DNA, an increase in the enthalpy variation with increasing complexity of surfactants (ala < pro < phe). This is believed to be due to the larger hydrophobicity of the proline group, when compared to the alanine group, as also indicated by the cmc values of the surfactants (Figure 1).

When surfactants with the ester linker are considered instead, and for most studied conditions, the surfactants with the proline head groups show a larger first relative rate constant (Figure 7). It should be noted, however, that the differences are small, increasing with the surfactant concentration and salt concentrations. For k_2, on the other hand, the values are nearly the same for ester-ala and ester-pro at the larger studied surfactant concentrations but are lower for ester-pro at lower surfactant concentrations. This indicates that the binding of

dx.doi.org/10.1021/jp301069t | J. Phys. Chem. B 2012, 116, 5831–5837

ester-pro surfactant to DNA and ester-pro micelle formation is slightly more favorable than that of ester-ala, for the reasons mentioned above. However, DNA condensation seems to occur at a lower (or equal, depending on surfactant concentration) rate for ester-pro.

CONCLUSION

Stopped-flow fluorescence has been used to monitor the kinetics of the association between DNA and cationic surfactants having different architectures, varying both the headgroup and the linker. We have additionally varied the surfactant-to-DNA charge ratio and the ionic strength. It was found that, for all the studied surfactants and conditions, the binding occurs in two steps. The two steps were attributed to the diffusion-controlled surfactant binding and micelle formation (k_1) and to DNA conformational changes (k_2). This was deduced from the increase in both relative rate constants with surfactant concentration and the decrease with salt concentration. The relative rate constants also provide information about the degree of binding of the surfactants to DNA, decreasing with a weaker binding. It was found that surfactants with weaker amide linker groups bind more strongly to DNA presenting also larger rates for DNA condensation, when compared to the surfactants with ester linker. The dependence of the relative rate constants on the headgroup of the surfactants (alanine vs proline) was found to be less obvious. The amide surfactants with proline headgroup showed a stronger interaction with DNA. This has been observed previously and is believed to be due to the more hydrophobic character of the proline group, which results in a decrease in both the cac and the cmc. Considering the ester surfactants, it is found that the same trend is followed for the first relative rate constant. The second relative rate constant, on the other hand, has the same value for ester-ala and ester-pro for large surfactant concentrations, but decreases for lower surfactant concentrations. This is an indication that binding of ester-pro surfactant to DNA and ester-pro micelle formation is more favorable, but DNA condensation seems to occur at a lower rate in the presence of ester-pro, when compared to ester-ala.

AUTHOR INFORMATION

Corresponding Author

*E-mail: rsdias@qui.uc.pt; fax: +351239827703 (R.S.D.). E-mail: bcpkd@iacs.res.in; fax:+913324732805 (P.K.D). E-mail: souvik@igib.res.in; fax: +911127667471 (S.M.).

Present Address

#Department of Applied Chemistry, Delhi Technological University, Delhi-110042, India.

Notes

The authors declare no competing financial interest.

ACKNOWLEDGMENTS

The Swedish International Development Cooperation Agency (SIDA), Council of Scientific and Industrial Research (CSIR young scientist award project), and Department of Science and Technology (DST fast track project), Government of India, New Delhi, are gratefully acknowledged for financial support. R.S.D. is also thankful to the Fundação para a Ciência e a Tecnologia, Portugal, for financial support through the program Ciência 2007.

REFERENCES

(1) Miller, A. D. *Angew. Chem., Int. Ed.* **1998**, *37*, 1769−1785.
(2) *Nonviral Vectors for Gene Therapy*; Huang, L., Huang, M.-C., Wagner, E., Eds.; Academic Press: San Diego, CA, 1999.
(3) *Pharmaceutical Prespectives of Nucleic Acid-Based Therapeutics*; Mahato, R. I., Kim, S. W., Eds.; Taylor and Francis: London, 2002.
(4) *DNA Interactions with Polymers and Surfactants*; Dias, R. S.; Lindman, B., Eds.; John Wiley & Sons: Hoboken, N.J., 2008.
(5) *Advances in Genetics: Non-Viral Vectors for Gene Therapy*, 2nd ed.; Huang, L., Huang, M.-C., Wagner, E., Eds.; Elsevier: San Diego, CA, 2005; Vol. *53*.
(6) Niidome, T.; Huang, L. *Gene Ther.* **2002**, *9*, 1647−1652.
(7) Mintzer, M. A.; Simanek, E. E. *Chem. Rev.* **2009**, *109*, 259−302.
(8) Yang, Z. R.; Wang, H. F.; Zhao, J.; Peng, Y. Y.; Wang, J.; Guinn, B. A.; Huang, L. Q. *Cancer Gene Ther.* **2007**, *14*, 599−615.
(9) Ahmad, A.; Evans, H. M.; Ewert, K.; George, C. X.; Samuel, C. E.; Safinya, C. R. *J. Gene Med.* **2005**, *7*, 739−748.
(10) Smith, P.; Lynden-Bell, R. M.; Smith, W. *Phys. Chem. Chem. Phys.* **2000**, *2*, 1305−1310.
(11) Zhang, S. B.; Xu, Y. M.; Wang, B.; Qiao, W. H.; Liu, D. L.; Li, Z. S. *J. Controlled Release* **2004**, *100*, 165−180.
(12) Kodama, K.; Katayama, Y.; Shoji, Y.; Nakashima, H. *Curr. Med. Chem.* **2006**, *13*, 2155−2161.
(13) Jadhav, V.; Maiti, S.; Dasgupta, A.; Das, P. K.; Dias, R. S.; Miguel, M. G.; Lindman, B. *Biomacromolecules* **2008**, *9*, 1852−1859.
(14) Jadhav, V. M.; Valaske, R.; Maiti, S. *J. Phys. Chem. B* **2008**, *112*, 8824−8831.
(15) Santhiya, D.; Dias, R. S.; Shome, A.; Das, P. K.; Miguel, M. G.; Lindman, B.; Maiti, S. *Langmuir* **2009**, *25*, 13770−13775.
(16) Dias, R.; Mel'nikov, S.; Lindman, B.; Miguel, M. G. *Langmuir* **2000**, *16*, 9577−9583.
(17) Maulik, S.; Chattoraj, D. K.; Moulik, S. P. *Colloids Surf. B* **1998**, *11*, 57−65.
(18) Grueso, E.; Roldan, E.; Sanchez, F. *J. Phys. Chem. B* **2009**, *113*, 8319−8323.
(19) Barreleiro, P. C. A.; Lindman, B. *J. Phys. Chem. B* **2003**, *107*, 6208−6213.
(20) Braun, C. S.; Fisher, M. T.; Tomalia, D. A.; Koe, G. S.; Koe, J. G.; Middaugh, C. R. *Biophys. J.* **2005**, *88*, 4146−4158.
(21) Wang, R. Y.; Ji, M. N.; Wang, R.; Shi, J. *Spectrochim. Acta A* **2008**, *71*, 1042−1048.
(22) Manzano-Ayala, H. R.; Romero, J. M. F.; Gomez-Hens, A. *Anal. Chim. Acta* **2009**, *632*, 109−114.
(23) Sambrook, J.; Fritsch, E. J.; Maniatis, T. *Molecular Cloning: A Laboratory Manual*; Cold Spring Harbor Laboratory Press: New York, 1989.
(24) Waring, M. J. *J. Mol. Biol.* **1965**, *13*, 269−282.
(25) Tonomura, B.; Nakatani, H.; Ohnishi, M.; Yamaguchiito, J.; Hiromi, K. *Anal. Biochem.* **1978**, *84*, 370−383.
(26) Le Pecq, J. B. *Methods Biochem. Anal.* **1971**, *20*, 41−86.
(27) Dasgupta, A.; Das, P. K.; Dias, R. S.; Miguel, M. G.; Lindman, B. *J. Phys. Chem. B* **2007**, *111*, 8502−8508.
(28) Hayakawa, K.; Santerre, J. P.; Kwak, J., C. T. *Biophys. J.* **1983**, *17*, 175−181.
(29) Shirahama, K.; Takashima, K.; Takisawa, N. *Bull. Chem. Soc. Jpn.* **1987**, *60*, 43−47.
(30) Holmberg, K.; Jönsson, B.; Kronberg, B.; Lindman, B. *Surfactants and Polymers in Aqueous Solution*, 2nd. ed.; John Wiley & Sons, Ltd:: West Sussex, U.K., 2003.
(31) Guldbrand, L.; Jönsson, B.; Wennerström, H.; Linse, P. *J. Chem. Phys.* **1984**, *80*, 2221−2228.
(32) Pisarcik, M.; Polakovicova, M.; Pupak, M.; Devinsky, F.; Lacko, I. *J. Colloid Interface Sci.* **2009**, *329*, 153−159.